Atmospheric nitrogen depositions in a highly human impacted area

Stefania Stevenazzi[1], Corrado A.S. Camera*[1], Marco Masetti[1], Roberto S. Azzoni[2], Elena S. Ferrari[1], Massimo Tiepolo[1]

[1] Dipartimento di Scienze della Terra "A. Desio", Università degli Studi di Milano, Milan, Italy

[2] Dipartimento di Scienze e Politiche Ambientali, Università degli Studi di Milano, Milan, Italy

* Corresponding author: corrado.camera@unimi.it

Abstract

Nutrients that fall on the ground from the atmosphere represent a minor component of the total nitrogen (N) input to soils, especially when compared to agricultural, civil and industrial inputs (i.e., sewage treatment plants or sewage systems, fertilizer and manure applications). However, integrating all nitrogen forms, processes and scales can represent a breakthrough challenge for the understanding and the management of the N cycle.

A monitoring experiment was set up to collect wet atmospheric depositions in a human impacted area with multiple land uses, representing different emission sources. Rainwater collection was executed in the surroundings of Milan, in northern Italy, starting from February 2017 to February 2019.

The presence of N compounds and their temporal variations in rainwater are consistent with pollution coming from local anthropogenic emission sources of nitrogen oxides and ammonia, mainly related to the use of the heating systems in the cold seasons and the spreading of fertilizers and manure on agricultural fields. Consequently, the total amount of N wet depositions range between 14 and about 30 kg/ha·yr in the study area.

As leaching of N compounds from soils generally increases at deposition rates higher than about 10 kg(N)/ha·yr, this work suggests that the N atmospheric input to soils could not be neglected when evaluating the impacts of N sources to terrestrial and aquatic ecosystems, as well as to groundwater resources. This highlights the need of wisely integrating air, soil and water policies for minimizing the risk to deteriorate surficial ecosystems and groundwater.

Keywords

Wet deposition, rainfall chemistry, ecosystem, ammonium, nitrate, Italy

Acknowledgments

The Authors wish to acknowledge the colleagues of the Department of Earth Sciences “A. Desio” of the University of Milan, for their help in collecting the rainwater samples, and the Italian Ministry of Education (MIUR) that partially supported this work through the project “Dipartimenti di Eccellenza 2017”.

1 Introduction

Changes in land cover and land use induced by anthropogenic activities are one key drivers in the modifications of precipitation chemical composition, which occurs from the incorporation of atmospheric gases and suspended particulate matter in water droplets (EEA, 2018). Nitrogen (N) and Sulphur (S) emissions in the atmosphere have large impacts on human health and ecosystems (Ochoa-Hueso et al., 2011; Buoli et al., 2018). Although some natural processes (biological and volcanic) can act as potential sources of N and S pollutants in the atmosphere, most of N and S emissions are closely related to anthropogenic activities, such as biomass burning, industrial activities, fertilizer applications and livestock wastes (Deusdará et al., 2017).

Nitrogen oxides (NO_x) and Ammonia (NH_3) are the two major forms of nitrogen emissions. NO_x and NH_3 react in the atmosphere to produce nitrate (NO_3^-) and ammonium (NH_4^+) aerosols. Sulphur is commonly injected in the atmosphere in a low oxidation state (e.g., SO_2), oxidised and shortly removed as sulphate (SO_4^{2-}) (e.g., Brimblecombe, 2003). All N-S compounds are removed from the atmosphere and deposited on the ground or aquatic surfaces by rain, hail or snow (i.e., wet deposition; Sutton et al., 2011). Identifying the chemical composition of wet depositions is a key issue to evaluate the potential impacts of pollutants on both surficial and subterranean ecosystems functionality (Xiao et al., 2013).

The rapid growth of N inputs from anthropogenic sources has become an important global environmental issue in many areas of the world (Galloway et al., 2008; Williams et al., 2017). Recent studies on nutrient budgets suggest that the atmosphere can be a significant source of nutrients that may even lead

to an excess of nutrients with respect to the critical loads sustainable by habitat classes (Grimshaw and Dolske, 2002; Meyer et al., 2015; Payne et al., 2013). Nitrogen provided by wet deposition is also suggested to be one of the main factor enhancing eutrophication processes by stimulating the growth of algae, which deplete oxygen and cause suffocation of fish and other aquatic organisms in water bodies (Schindler, 2006; Naselli-Flores, 2010). Forest decline has been reported worldwide as one of the negative effects of increasing N deposition in ecosystems (Kennedy, 2001). Another worldwide environmental issue is related to excess NO_3^- transport into groundwater, which damages its quality (Ham and Tamiya, 2006; Ochoa-Hueso et al., 2011). Airborne NO_3^- can also affect background values of contaminants in non-pristine areas. This is a recurrent controversial point, especially in urban areas where it can be hard to determine the base level of contamination of compounds that have both natural and anthropogenic sources (Panno et al., 2006). The chemistry of wet deposition is thus a key issue in quantifying rainfall contribution to groundwater quality and therefore in defining specific background values of contaminants in it. This is particularly relevant for vulnerable aquifers exposed to non-point sources of contamination (Kim et al., 2015).

The implementation of Italian environmental directives has decreased in the last 30 years air pollution and acid rain of the country (Rogora et al., 2016). Notwithstanding, recent measures from satellites Sentinel-5P/Tropomi (ESA, 2019a; ESA, 2019b) and Aura/OMI (NASA Hyperwall, 2018) revealed that the atmosphere in the Po Plain (Northern Italy) is still deeply impacted by NO_2 pollution.

This study focuses on a sector of the Po Plain that can be considered an excellent test area, due to the presence of different land uses and land covers, for the fulfilment of multiple aims: a) the characterization of the rainfall chemistry in a high anthropogenic impacted area with multiple land uses; b) the development of maps for wet nitrogen deposition; c) the evaluation of the implication of wet nitrogen deposition on surficial and subterranean ecosystems.

2 Study area

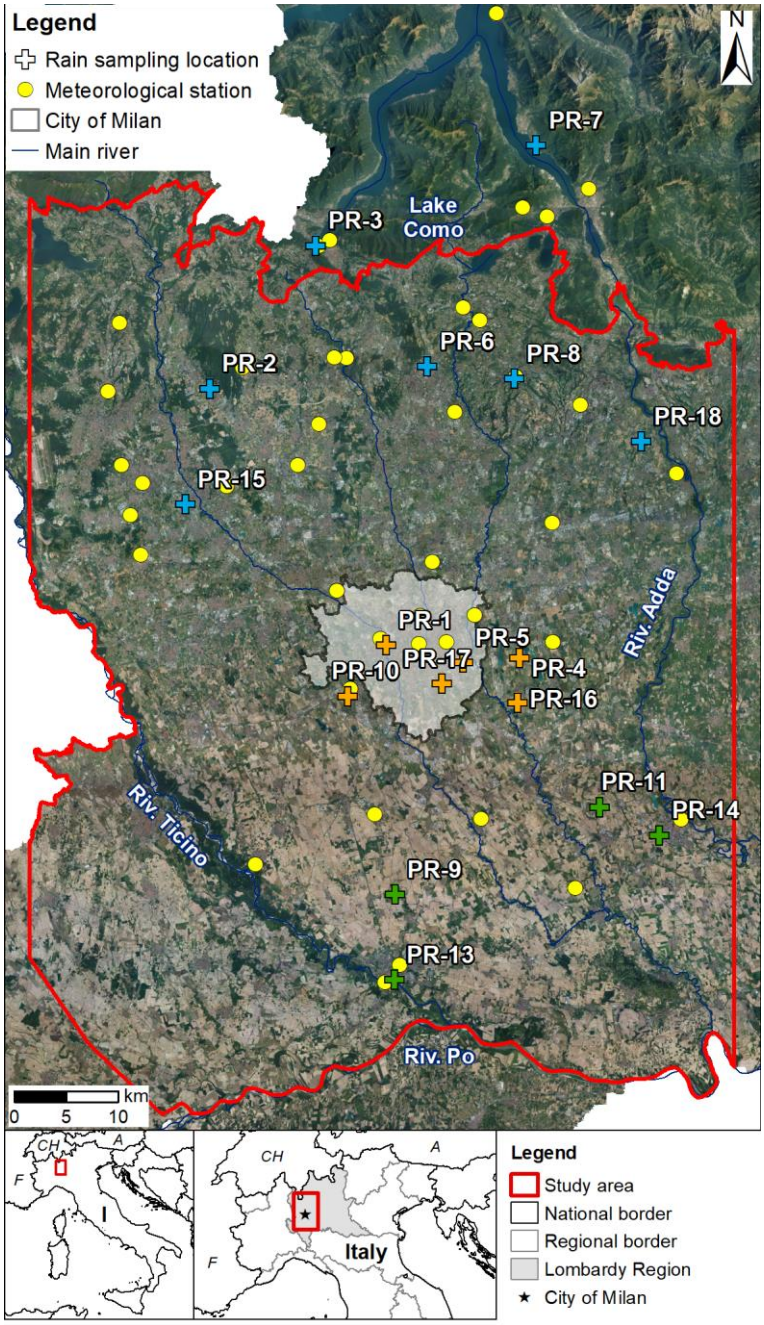

Figure 1 – Location of the study area with highlighted the regional (ARPA) meteorological monitoring network and the 17 rainfall sampling sites (crosses, see details in Table 1). Blue, orange and green crosses represent northern, central and southern sites, respectively.

The investigated area (about 3000 km²) is located in northern Italy, in the western sector of Lombardy Region, within the Po Plain (Figure 1). The Plain is closed off by the Alps to the north and west and by the

Apennines to the south. Such topography, under high-pressure systems, favours stagnant atmospheric conditions and the recirculation of air through the typical mountain-valley breeze (Dosio et al., 2002). The local atmospheric circulation patterns, in combination with elevated anthropogenic emissions, make the Po Plain a major "hot spot" of nitrogen dioxide in the world (e.g., Ordoñez et al., 2006; Stevenazzi et al., 2015; NASA Hyperwall, 2018; ESA, 2019a; ESA, 2019b). Potential sources of atmospheric pollutants in the area are agricultural activities (e.g., breeding farms, manure storages, fertilization of fields and plants) and technological activities in urban areas (e.g., residential and commercial combustion, industrial production, road traffic and air transport) (Carnevale et al., 2008; Sutton et al., 2011; ISPRA, 2016; Van Damme et al., 2018).

Although the study area is relatively small, the annual precipitation is highly variable. It ranges from 900 mm in the southern part to more than 1700 mm in the northern portion (data covering the period 1891-1990, Ceriani and Carelli, 2003). The major factor affecting rainfall variability is the orography of the pre-alpine ridges, which forces the condensation of the water vapour in the area of pre-alpine lakes (Brunetti et al., 2000). According to the Koppen Geiger classification (Peel et al, 2007), the study area can be divided in two different zones: i) a temperate oceanic climate characterizing the sites located in the proximity of Como Lake and ii) a humid subtropical climate (Cfa), typical of the other sites.

Based on environmental characteristics, urban patterns and main anthropogenic activities, the study area can be further subdivided into three sectors (Figure 1): a) a medium-to-high urbanized area with natural green lands as the foothills of the Alps in the northern sector; b) a highly urbanized and industrialized area in the central sector, represented by the city of Milan and its suburbs; c) an agricultural area with scattered cities and towns in the southern sector.

The study area is covered by a network of 45 meteorological stations with a nearly uniform spatial distribution that is managed by the Regional Environmental Agency (Figure 1, ARPA Lombardia, http://www.arpalombardia.it). Meteorological stations measure hourly: amount and intensity of precipitation, air temperature and pressure, wind direction and velocity, solar radiation.

3 Measurements and methods

3.1 Rainwater sampling and laboratory analyses

Wet atmospheric depositions were collected at 17 sampling points (Figure 1, Table 1). Rainwater was collected during almost each single rainfall event at all the sites, starting from February 2017 until February 2019. Sixteen precipitation events were monitored and 155 rainwater samples were collected, involving, on average, 10 sites each time. Limitations to the collection of rainwater samples were mostly related to a) not homogeneous spatial distribution of a precipitation event; b) low frequency of precipitation events during the monitoring period; c) availability of volunteers collecting rainwater samples. Rainwater collection was organized based on a participatory activity involving the colleagues of the Department of Earth Sciences, therefore the monitoring network was reorganized in conjunction with students or colleagues leave or arrival. However, the collection network always had at least 10 active points, and attention was given to have the three sectors of the study area well represented (see Table 1 for details). Rainwater samples were collected with a sampling device consisting of a 250 mL glass container with a metal lid (jam jar style) and a 20-cm diameter plastic funnel. In addition, each volunteer was provided with a memorandum containing the instructions for rainwater collection. Prior to each rainwater sampling, the glass containers and the plastic funnels were washed with deionized (15.0 MΩcm) and high purity (18.0 MΩcm) water. For sampling, the device was exposed at the beginning of the precipitation event until it was at least 1/4 full, or until the end of the event if the 1/4 amount was not reached. Then, the opening of the device was covered with a plastic wrap and closed with the metal lid. The volunteer took note of the beginning and ending of the collection period, in terms of date and time (dd/mm/yyyy hh:mm). The glass container was stored at 4°C in a refrigerator until its return to the laboratory.

Rainwater samples were analysed for pH, electric conductivity (EC), ammonium, major cations (calcium, magnesium, sodium, potassium) and major anions (sulphate, nitrate, chloride, fluoride). All the analyses were performed on filtered samples (2-14 μm). pH and EC were measured with a pH meter and a conductivity meter (MultiLine P3 pH/LF-Set, by WTW), respectively. Cations were determined in part by microwave plasma atomic emission spectroscopy using an Agilent 4100 MP-AES and in part by ion chromatography using

a Dionex ICS-900. The agreement between the two techniques was established following Bland and Altman (1999) and results are reported in the Appendix 1. Ion Chromatography was also used for the determination of anions concentrations in all samples. All physico-chemical analyses were conducted within 72 hours from the collection event. To prevent loss of ions due to precipitation/dissolution reaction or evaporation before the analyses, samples were stored at 4°C in a refrigerator. Blank samples were analysed in each analytical run to monitor possible contamination during the transport, filtration, and preservation of samples.

Table 1 – Characteristics of the sampling sites. Cat: category of the site according to its location (North = northern site, Centre = central site, South = southern site).

Collecting point ID	Cat.	City	Province	Altitude (m a.s.l.)	Collecting period	Mean total yearly precipitation (mm)	Number of samples
PR-1	Centre	Milan	Milan	122	Feb 2017 – Feb 2019	1000	10
PR-2	North	Locate Varesino	Como	278	Feb 2017 - Feb 2019	1350	15
PR-3	North	Como	Como	247	Oct 2017 - Feb 2019	1450	6
PR-4	Centre	Peschiera Borromeo	Milan	107	Feb 2017 - Feb 2019	950	10
PR-5	Centre	Milan	Milan	110	Feb 2017 - Feb 2019	1000	9
PR-6	North	Carugo	Como	280	Feb 2017 - Oct 2017	1400	6
PR-7	North	Abbadia Lariana	Lecco	250	Oct 2017 - Feb 2019	1650	7
PR-8	North	Casatenovo	Lecco	376	Feb 2017 - Feb 2019	1300	14
PR-9	South	Giussago	Pavia	87	Feb 2017 - Apr 2018	850	10
PR-10	Centre	Corsico	Milan	115	Feb 2017 - Feb 2019	950	10
PR-11	South	Tavazzano con Villavesco	Lodi	84	Feb 2017 - Feb 2019	900	10
PR-13	South	Pavia	Pavia	67	Feb 2017 - Feb 2019	800	13
PR-14	South	Lodi	Lodi	79	Feb 2017 - Feb 2019	850	12
PR-15	North	Legnano	Milan	209	Mar 2017 - Apr 2017	1100	2
PR-16	Centre	Peschiera Borromeo	Milan	98	Sep 2017 - Feb 2019	950	11
PR-17	Centre	Milan	Milan	110	Jan 2018 - Jul 2018	1000	5

PR-18	North	Cornate d'Adda	Milan	235	Mar 2018 - Feb 2019	1100	5

3.2 Characterisation of rainfall chemistry

A series of descriptors (a-e) were used to check data quality (a-b) and to perform the characterisation of rainfall chemistry (c-e):

a) the ionic balance;

b) the electric conductivity balance;

c) the marine inputs (sea salt and non-sea salt fractions);

d) the neutralization factor;

e) descriptive statistics for ionic concentrations, EC and pH values: arithmetic mean, volume weighted mean, median, minimum and maximum values and standard deviation.

Details on procedures and equations are reported in Appendix 2.

Nitrogen compounds, as nitrate and ammonium, were furtherly investigated according to their spatial distribution and temporal variation. Similarities or differences in the spatial distribution of N compounds are related to the location of the collecting stations in the three sectors of the study area (northern, central and southern sectors). Whereas, temporal variations of N compounds are related to the season when rainwater samples have been collected.

3.3 Estimating nitrogen wet deposition

Maps of deposition of nitrate (NO_3^-) and ammonium (NH_4^+) were obtained by multiplying precipitation maps with concentration maps (e.g., Rogora et al., 2016). A mean annual precipitation map was obtained interpolating annual cumulative precipitation measurements, retrieved from the meteorological network of the Regional Environmental Protection Agency (ARPA Lombardia, http://www.arpalombardia.it), for the years 2017 and 2018 and averaging the two resulting layers. The interpolation was performed through kriging technique.

The concentration maps for NO_3^- and NH_4^+ were calculated as functions of latitude, longitude and altitude, following a procedure proposed by Steingruber (2015) based on multiple linear regression analyses:

$$C = m_{long} \cdot longitude + m_{lat} \cdot latitude + m_{alt} \cdot altitude + C_0 \quad \text{(Eq. 1)}$$

where C is the volume weighted mean of concentration values, C_0 is the intercept, m_{long}, m_{lat}, and m_{alt} are the linear regression coefficients. Longitude, latitude and altitude are given in m. In this study, longitude and latitude coordinates refer to the WGS 1984 – UTM zone 32 Nord projection, while altitude is derived from the digital terrain model provided by Regione Lombardia (http://www.geoportale.regione.lombardia.it/), with a resolution of 20 m × 20 m. Before the application of Steingruber's method (2015), a principal component analysis (PCA) was performed to identify similarities of observations and parameters (i.e., chemical and geographic parameters) and verify the effective correlation between geographical coordinates and rainfall chemistry. PCA was performed for volume weighted means of the main chemical parameters (pH, EC, main anions and cations) over the entire collection period (February 2017 – February 2019).

Lastly, nitrate and ammonium deposition maps were transformed in nitrogen equivalent maps. Deposition amounts are expressed as kg per hectare per year (kg ha^{-1} yr^{-1}) to be equivalent to the unit used for agricultural loadings, where 1 kg (N) ha^{-1} yr^{-1} is equivalent to 4.426 kg (NO_3^-) ha^{-1} yr^{-1} or 1.288 kg (NH_4^+) ha^{-1} yr^{-1}. The resulting maps were added together to obtain a single map of total nitrogen depositions.

4 Results

4.1 Rainwater chemistry

Results indicate that sample contamination is negligible. Most of the analyses satisfy the requirements of quality assurance (Figure 2). Part of these samples showing a cation deficient were analysed with the sole MP-AES that does not measure ammonium. Samples with anion deficit may contain short-chain organic acids, which were not among the detected anions (Mosello and Tartari, 1992).

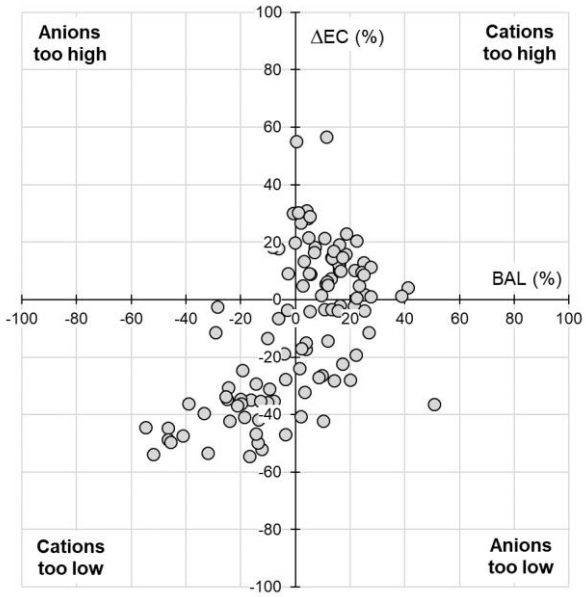

Figure 2 – Comparison between charge balance (x-axis) and ΔEC (y-axis) of all samples.

The acidity of rainwater mainly depends on the relative abundance of the dominant acids (i.e., H_2SO_4, HNO_3 and organic acids) and alkaline species (e.g., NH_3, $CaCO_3$). Pure water in equilibrium with atmospheric CO_2 has a pH of 5.65. When acidification occurs, pH values may be as low as 4 (Charlson and Rhode, 1982; Galloway et al., 1982). Rainfall samples collected in the period 2017-2019 in the study area show pH values ranging between 4.4 and 7.3 (Table 2), with more than 40% of the samples characterized by a pH in the range 6.0 – 6.5 (Figure 3a).

The EC of precipitation reflects the total soluble components. Generally, low EC values (< 10 μS/cm) reflect better atmospheric environmental quality, whereas high EC values (> 60 μS/cm) indicate a substantial impact of anthropogenic pollution on the atmospheric environment (Yang et al., 2012). EC of collected rainfall samples varies between 4 μS/cm and 252 μS/cm (Table 2). An inverse correlation between the EC of rainwater and the amount of sampled rainfall is observed (Figure 3b). It is illustrated that precipitation samples with high EC may imply small rainfall amount (< 1.6 mm). Increasing rainfall amounts seem to enhance the dilution of the particulate matter and gaseous pollutants; the EC of rainwater consequently shows a descending trend. However, high EC (> 60 μS/cm) have been also detected in samples characterized by large rainfall amounts. This fact is related to local pollution conditions during the precipitation event.

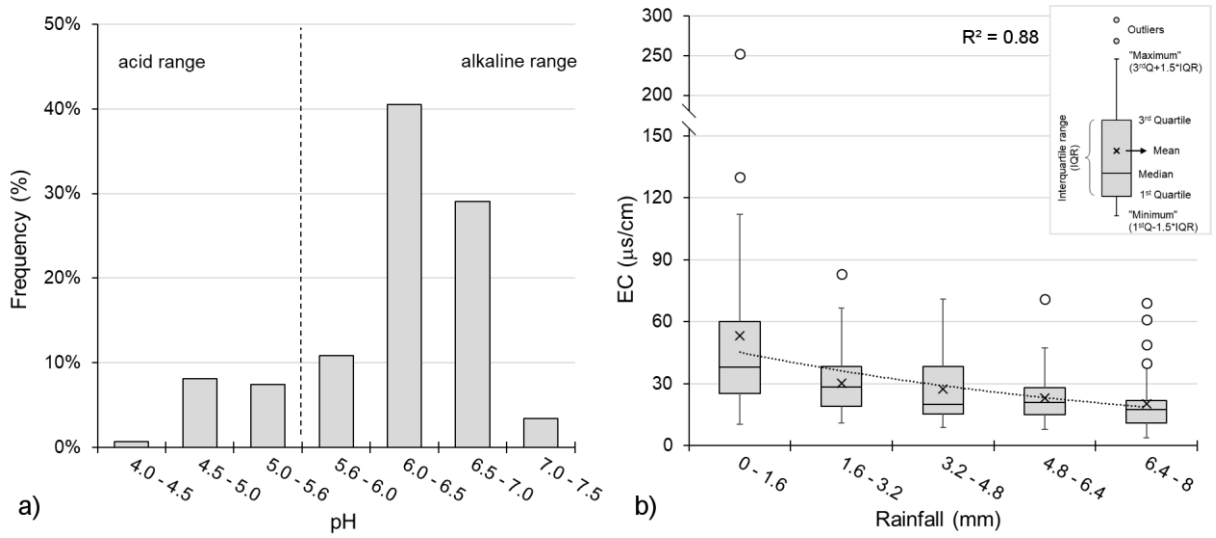

Figure 3 – a) Frequency distribution of pH during the sampling period and b) relation between sampled rainfall amount and EC in precipitation. The limit to 8.0 mm as maximum amount of rainwater is related to the maximum volume of the glass container. The explanation of a box and whisker plot graph is represented in the upper right panel.

Table 2 – Rain ion concentration statistics. N is the number of over-the-detection limit values. The minimum water volume for EC and pH measurements is 20 mL. The total number of samples is 155.

	Unit	N	Vol. weighted mean (VWM)	Arithmetic mean	Minimum	Median	Maximum	Standard deviation	Instrument
EC	to 25°C, mS/cm	148	24.2	28.8	4.0	21.3	252.0	26.6	Conductivity meter
pH	to 25°C	148	6.3	6.2	4.4	6.4	7.3	0.6	pH meter
F^-	mg/L	26	0.2	0.2	0.1	0.2	0.9	0.2	Ion Chromatography System (ICS)
Cl^-	mg/L	155	1.3	1.9	0.2	1.2	25.8	2.7	
NO_2^-	mg/L	138	0.2	0.3	0.1	0.2	4.0	0.4	
NO_3^-	mg/L	155	3.7	4.7	1.0	2.9	41.4	5.3	
SO_4^{2-}	mg/L	154	2.1	2.6	0.7	1.9	26.1	2.8	

PO_4^{2-}	mg/L	3	2.0	1.7	0.3	1.0	3.9	1.9	
Ca^{2+}	mg/L	51	1.1	1.2	0.2	0.9	4.8	1.0	Microwave Plasma - Atomic Emission Spectroscopy (MP-AES)
Mg^{2+}	mg/L	51	0.2	0.2	0.0	0.1	1.9	0.3	
Na^{+}	mg/L	51	0.5	0.6	0.1	0.5	1.9	0.4	
K^{+}	mg/L	51	0.4	0.5	0.0	0.2	3.0	0.7	
Ca^{2+}	mg/L	100	1.4	1.7	0.2	0.9	30.6	3.3	Ion Chromatography System (ICS)
Mg^{2+}	mg/L	97	0.1	0.2	0.0	0.1	2.3	0.3	
Na^{+}	mg/L	100	0.5	0.8	0.1	0.3	12.0	1.5	
K^{+}	mg/L	100	0.4	0.5	0.0	0.2	5.1	0.7	
$NH4^{+}$	mg/L	99	1.9	2.2	0.2	1.7	7.2	1.7	

The sea salt fraction (SSF) and the non-sea salt fraction (NSSF) of marine salts are shown in Table 3. A marine contribution is clear for chloride ion (SSF = 68.7 %). The high NSSF (higher than 90 %) suggests terrestrial (crustal dust, road dust, plant matter) or anthropogenic (vehicle or industrial emissions, biomass burning) sources for Ca^{2+}, K^{+} and SO_4^{2-}. The SSF for Mg^{2+} is only slightly higher than the NSSF and thus it is difficult to define a preferential terrestrial or marine origin.

Table 3 – Sea salt water contribution (SSF) and non-sea water contribution (NSSF). In bold are indicated the largest contributions.

	Ions				
	Ca^{2+}	**Mg^{2+}**	**K^{+}**	**Cl^{-}**	**SO_4^{2+}**
SSF (%)	2.1	59.4	7.7	**68.7**	6.5
NSSF (%)	**97.9**	40.6	**92.3**	31.3	**93.5**

The neutralization factor (NF) of Ca^{2+}, Mg^{2+}, K^{+} and NH_4^{+} cations by the NO_3^{-} and SO_4^{2-} anions are reported in Table 4. NH_4^{+} and Ca^{2+} show the highest NF (0.95 and 0.66, respectively) and are thus the major

contributors to the neutralization of the main acids (Table 4). K^+ and Mg^{2+} follow with nearly comparable NF. The balance between the acid and alkaline ions generally reflects the measured pH (Figure 4). Samples with acid ions concentration slightly higher than the alkaline ions are those with the lowest pH (less than 5). By contrast, samples with concentration in alkaline ions higher than the acidifying ions have pH values higher than 6.5.

Table 4 – Neutralization factors (NF).

	Ions			
	Ca^{2+}	**Mg^{2+}**	**K^+**	**NH_4^+**
NF	0.66	0.12	0.13	0.95

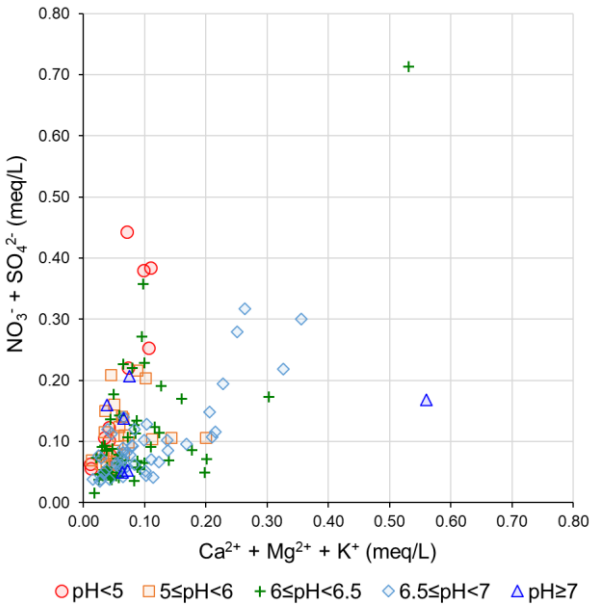

Figure 4 – Acidification process: relationship between the sum of acidifying anions (NO_3^- and SO_4^{2-}) and alkaline cations (Ca^{2+}, $Mg^{2+}$and K^+). Rainwater samples have been categorized according to the measured pH: pH < 5 (red circles), 5 ≤ pH < 6 (orange squares), 6 ≤ pH < 6.5 (green crosses), 6.5 ≤ pH < 7 (light blue diamonds), pH ≥ 7 (blue triangles).

Nitrogen compounds, as nitrate and ammonium, are the most abundant components in rainwater samples (Figure 5). Ca^{2+} is the dominant base cation followed by Na^+, Mg^{2+} and K^+. The rain chemical

composition is a function of the prevalent land use destination of the sampling area (urban and agricultural), as well as the local domestic, commercial or industrial activities present in the area. The abrasion of streets and sidewalks, the weathering of plasters, as well as building, industrial and agricultural activities are a major source for Ca^{2+} (Lee et al., 1999). The terrestrial origin for K^+ can be related to the dissolution of K-silicates in soil dust, possibly enriched in K-fertilizers (Panettiere et al., 2000), or to the combustion of wood for residential heating or agricultural fires (i.e., biomass burning; Amato et al., 2016; Rattigan et al., 2017). Sulphate and chloride are the most abundant anions after nitrate. The presence of SO_4^{2-} in rainwater reveals SO_2 atmospheric pollution from vehicles or power generator plants (Vet et al., 2014; EMEP/CEIP, 2018). As previously outlined, the major fraction of chloride in rainwater derive from sea salts particles in the atmosphere (SSF[Cl^-] = 68.7 %, Table 3). The remaining 31.3% of NSSF for Cl^- has local anthropogenic origin likely related to emissions from domestic wood combustion or paper industry (Celle-Jeanton et al., 2009; Deusdará et al., 2017).

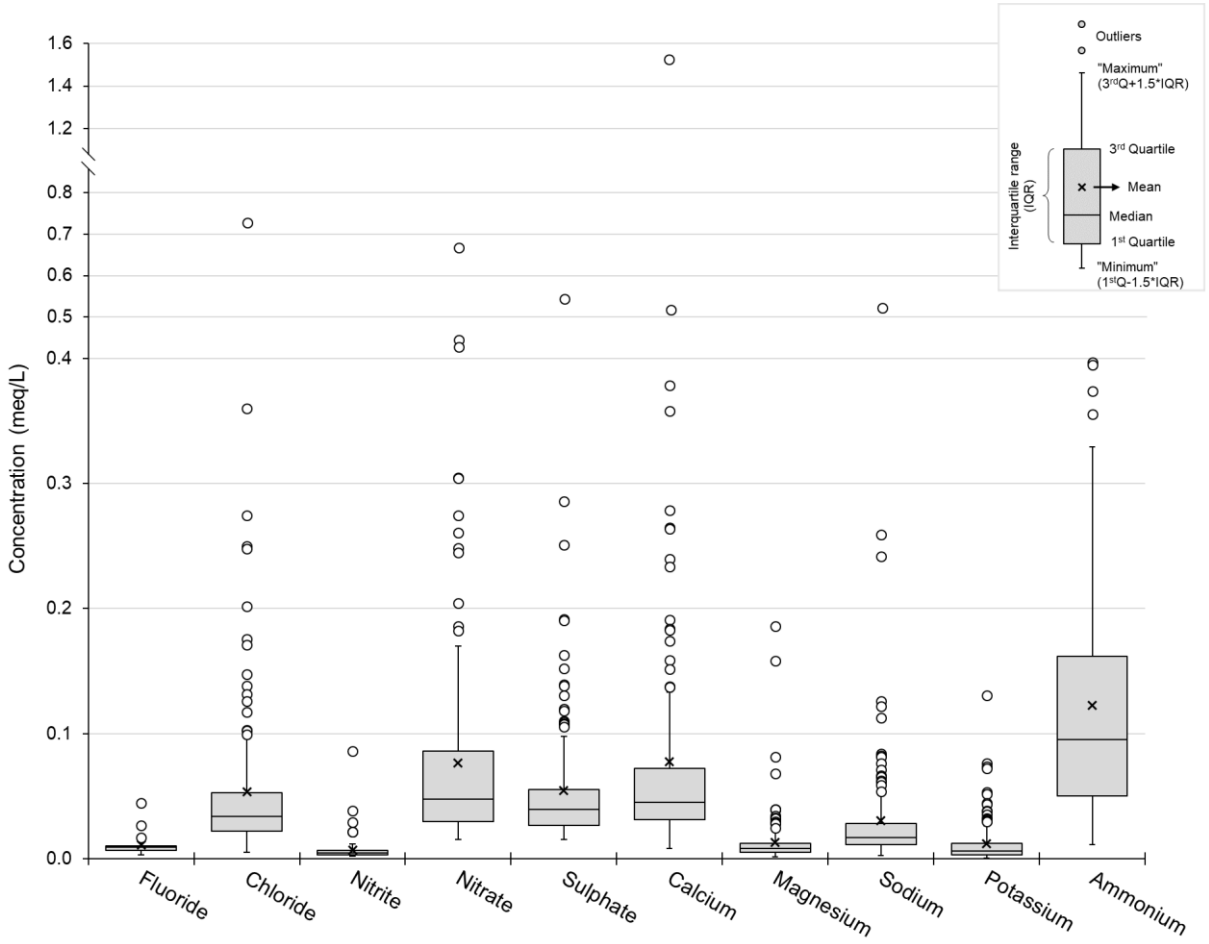

Figure 5 – Whisker and box plots of the major anions and cations concentrations. The explanation of a box and whisker plot graph is represented in the upper right panel.

The presence of NO_3^-, NO_2^- and NH_4^+ in rainwater confirms that pollution is coming from local anthropogenic emission sources of NO_x and NH_3. The major contributors of NO_x emissions in the study area are road transport, residential and commercial combustion, industrial production, followed by power generation, and air transport (Ordoñez et al., 2006; Carnevale et al., 2008; Sutton et al., 2011). NH_3 emissions mainly derive from agricultural activities - such as intensive animal farming (either in the form of open feedlots or within enclosed housings) and the application of manure and mineral fertilizer to the fields - and industrial emitters - such as plants producing NH_3-based fertilizers (Sutton et al., 2011; Van Damme et al., 2018). Nitrate and ammonium concentrations in the rainfall samples decrease northwards (Figure 6 a, b). This dependence can be a consequence of: a) the intensity of the precipitation events, b) the proximity to

the main emission sources, c) local meteorological conditions or particular landscape characteristics (natural or anthropic).

Precipitation events in the study area are mainly related to air masses originated from the Mediterranean Sea, which move over the Po Plain and collide with the Alps (Steingruber, 2015). The amount of precipitation increases from the plain to the mountain ridge, northward (ARPA Lombardia, http://www.arpalombardia.it; Ceriani and Carelli, 2003) and thus may cause a progressive dilution of pollutants, as already outlined in Figure 3b.

The main emission sources of N compounds in the atmosphere are located in the central and southern sectors of the study area, thus supporting the northwards decreasing of pollutants. As described in §2 (Figure 1), the central sector is characterized by the presence of the urban agglomeration of Milan, the suburban areas with lots of residential and commercial buildings and high traffic roads, which cause elevated NO_x emissions. Instead, the southern sector is characterized by large agricultural fields and animal farms, which cause high NH_3 emissions.

Point emission sources, as the Linate-Milan Airport located at the east side of Milan, and industrial activities in the northern side of the city have a remarkable impact on a local scale (Gómez-Carracedo et al., 2015). Moreover, local landscape characteristics, as skyscrapers and tall buildings, may behave as obstacles to air circulation (i.e., street canyons, Berkowicz et al., 1996), causing high variable concentrations in rainwaters in the central sector.

Time-dependent variations of N compounds have been observed during the monitoring period. The heating systems of residential and commercial buildings active in the cold season (15th October – 15th April) and emitting NO_x gases in the atmosphere account for the higher NO_3^- concentrations in rainwater observed during autumn and winter seasons (Figure 6c). The spreading of fertilizers and manure on agricultural fields during the fertilization periods is at the origin of the high concentrations of NH_3 in the atmosphere and, consequently, high concentrations of NH_4^+ in rainwaters (Figure 6d). The Regions in the Po Plain follow the EU Directive regulations on air quality (2008/50/EC) through an agreement for the control of atmospheric emissions during the cold seasons (1st October – 31st March, 151 days). According to this agreement, manure

spreading is regulated every three days based on weather forecasts (ERSAF, www.ersaf.lombardia.it). This allowed to recognize consistent temporal relationships between manure spreading and rainfall chemistry during autumn and winter (Figure 6e, f).

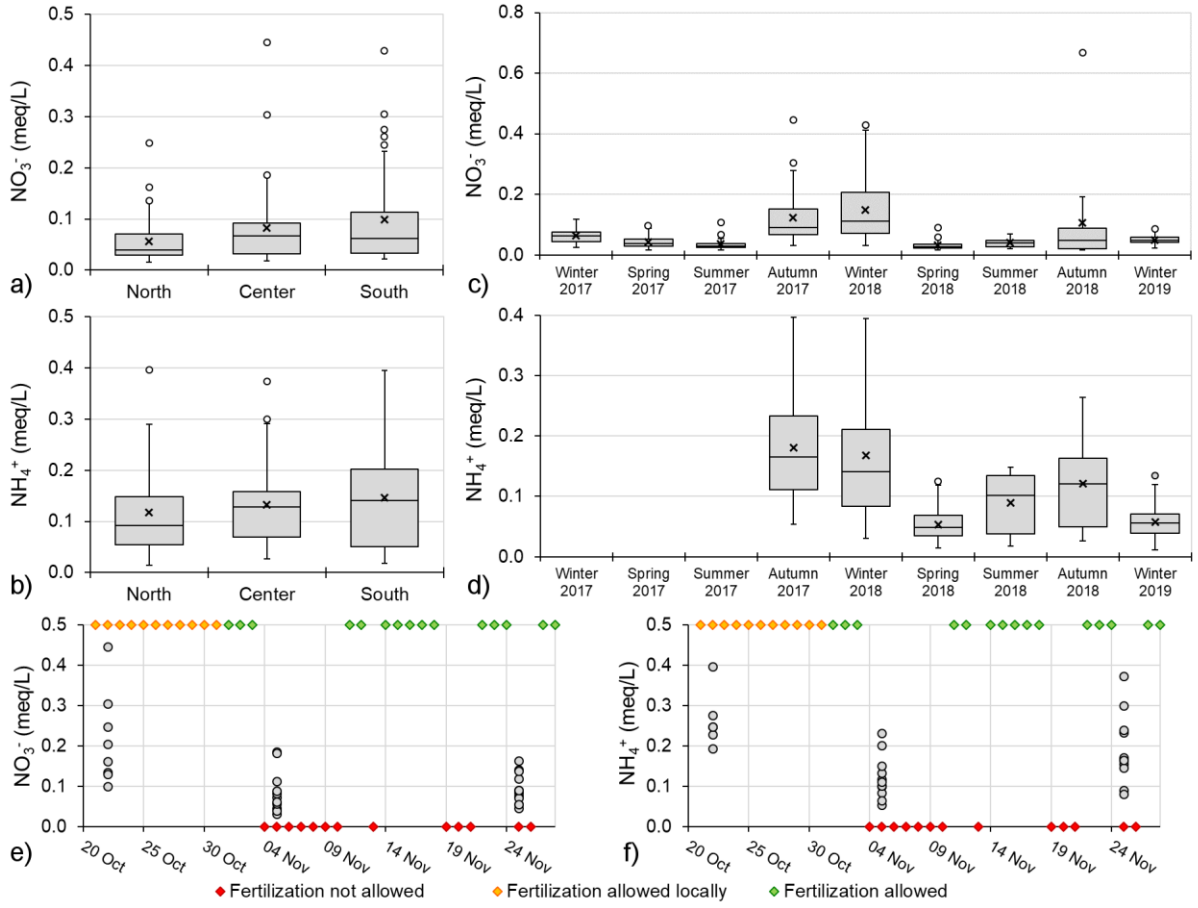

Figure 6 – Spatial (a, b) and temporal (c, d) patterns of nitrate and ammonium ions in rainwater samples. Nitrate (e) and ammonium (f) concentrations in rainwater samples (Sampling n. 7, 8 and 9, grey dots) compared to days when fertilization is allowed (green diamonds), partially allowed (yellow diamonds) or not allowed (red diamonds).

4.2 Wet inorganic nitrogen deposition

The estimation of the wet nitrogen deposition over an area is a strategical support for many regulators and policymakers: i) people engaged in agriculture are allowed to develop precision farming strategies for optimizing crop yield and profit and for minimizing potential environmental damage; ii) land managers can

use data for the protection of surficial water bodies in natural and managed ecosystems; iii) groundwater managers can determine background values of nitrates and understand the actual impact of point sources of contamination. The study area is excellent to test and evaluate all these problems.

4.2.1 Principal component analysis

The results of the PCA show that the first two principal components are able to capture most of the variance of the correlation matrix, 68 %. It also appears that most variables are very well described by the combination of the first two principal components, as the loadings of the variables are close to the circle of correlations (Figure 7a). Data show that latitude and elevation are closely related, likely because in the study area altitude usually increases with latitude. Most of the chemical parameters (i.e., nitrate, nitrite, ammonium, sulphate and base cations) correlate negatively with latitude and elevation. The negative correlation with latitude (Figure 6a, b) is related to the mechanism at the origin of rainfall in the studied area. Precipitation events in the study area are mainly determined by warm, humid air masses originating from the Mediterranean Sea, passing over the Po Plain and colliding with the Alps (Steingruber, 2015). Nitrate, ammonium and sulphate concentrations decrease northward as the distance from their main emission sources increases. For NO_x and SO_2 the emission source is the urban area of Milan, while for NH_3 the emission source is the agricultural district in the southern sector of the study area.

A clear correlation between the main chemical parameters (i.e., nitrate, nitrite, ammonium, and base cations) and longitude is not evident. In addition, longitude is poorly represented in both PC1 and PC2.A positive correlation between electric conductivity (EC) and concentrations of the main ions is confirmed by their close location in the circle of correlation. Instead, a slightly negative correlation between pH and concentrations of the main ions could be explained by the non-balance between acid and base ions (Figure 2).

Factor score plots show how collecting sites are correlated to each other with respect to their variables (Figure 7b). Collecting sites with similar characteristics are located close to each other. Most of the clusters of collecting sites reflect the distribution in the three main sectors (north, central and south). However, some sites differ from their respective groups: a) PR-1 differs from the central sites; b) PR-5 and PR-16 are located

very close to each other, highlighting similar characteristics, but very far from the central and southern clusters, respectively. In general, these collecting sites represent outliers of the respective sectors. Local emission conditions of the areas adjacent to the collecting site can be at the origin of the peculiar behaviour. For example, PR-5 and PR-16 sites are located in the East side of the city of Milan close to the Milan Linate Airport, which represents a peculiar emission point. PR-6 and PR15 were excluded from the PCA because of the absence of data regarding ammonium concentrations.

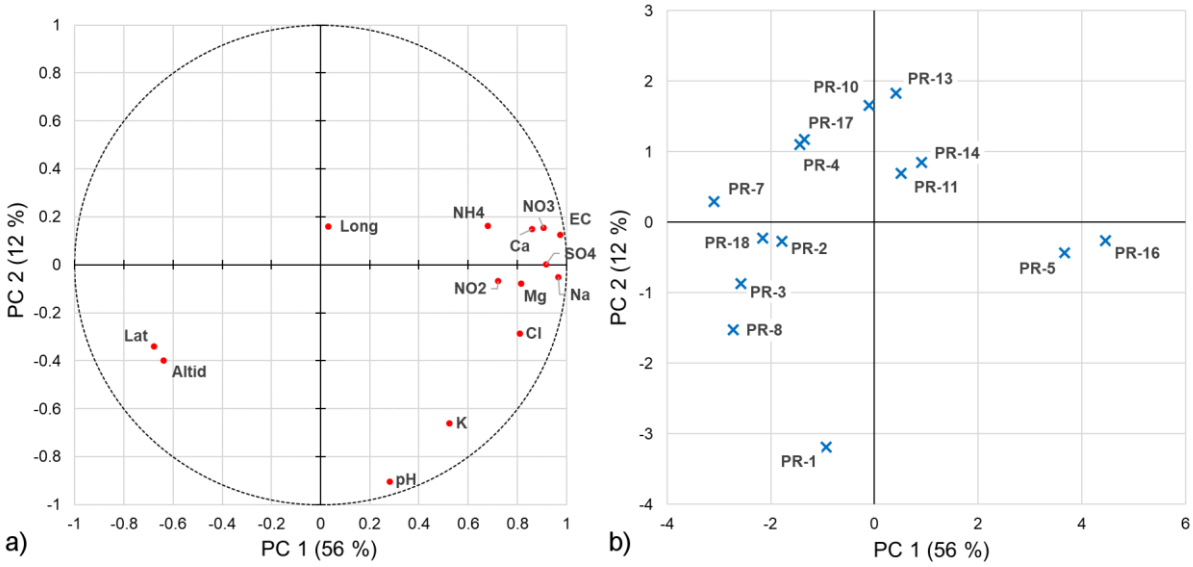

Figure 7 – a) Circle of correlation and plot of the loadings of the variable with principal components 1 and 2. b) Factor scores of the collecting points plotted on the principal components 1 and 2. The percentage values shown in the axes refer to the percentage amount of the variance captured by the component.

4.2.2 Multiple regression analysis

The results of the PCA suggest the possibility of developing a multiple regression model with latitude and altitude for NO_3^- and NH_4^+ concentrations. Differently respect to Steingruber method (2015), longitude has no clear correlation with the chemical parameters, according to PCA results. For this reason, longitude has not been included in the multiple regression analyses and Equation 1 has been changed accordingly:

$$C = m_{lat} \cdot \text{latitude} + m_{alt} \cdot \text{altitude} + C_0 \qquad \text{(Eq. 2)}$$

where C is the volume weighted mean of concentration values, C_0 is the intercept, m_{lat}, and m_{alt} are the linear regression coefficients. The linear regression coefficients of Equation 2 for nitrate and ammonium and the values describing statistical significance of the regression model are reported in Table 5.

Table 5 – Results from multiple regression analysis for nitrate and ammonium. r^2 = coefficient of determination, F = F-statistic, p = p-value, α = level of significance.

Parameter	m_{lat}	m_{alt}	C_0	r^2	F	p	α
	mg L^{-1} m^{-1}	mg L^{-1} m^{-1}	mg L^{-1}				
Nitrate	-9.11×10^{-6}	–0.00395	50.4	0.35	3.26	0.074	0.10
Ammonium	-9.42×10^{-6}	–0.00012	49.3	0.29	2.27	0.149	0.15

4.2.3 Nitrogen deposition maps

Deposition maps of N-NO_3^- and N-NH_4^+ are shown in Figure 8. Despite pollutant concentrations decrease with the increase of latitude and altitude (§ 4.2.1), rainfall amount increases (ARPA Lombardia, http://www.arpalombardia.it; Ceriani and Carelli, 2003). Therefore, nitrogen depositions expressed as N-NO_3^- and N-NH_4^+ increase northward with ammonium depositions often higher than those of nitrate. The total nitrogen deposition map is shown in Figure 9. Total N depositions range from 14 to about 30 kg (N) ha^{-1} yr^{-1}, with the lowest depositions occurring in the south-western area and the highest depositions in the north-eastern area, close to the city of Milan. This result confirms other estimates on global N depositions, which affirms that in large regions of the world average N deposition rates exceed 10 kg (N) ha^{-1} yr^{-1}, moreover, this value is an order of magnitude greater compared with natural rates (Galloway et al., 2008). These results are in agreement with those (20 and 25 kg (N) ha^{-1} yr^{-1} in the period 2000–2002) obtained by Rogora et al. (2012) for the neighbouring area of Lake Maggiore.

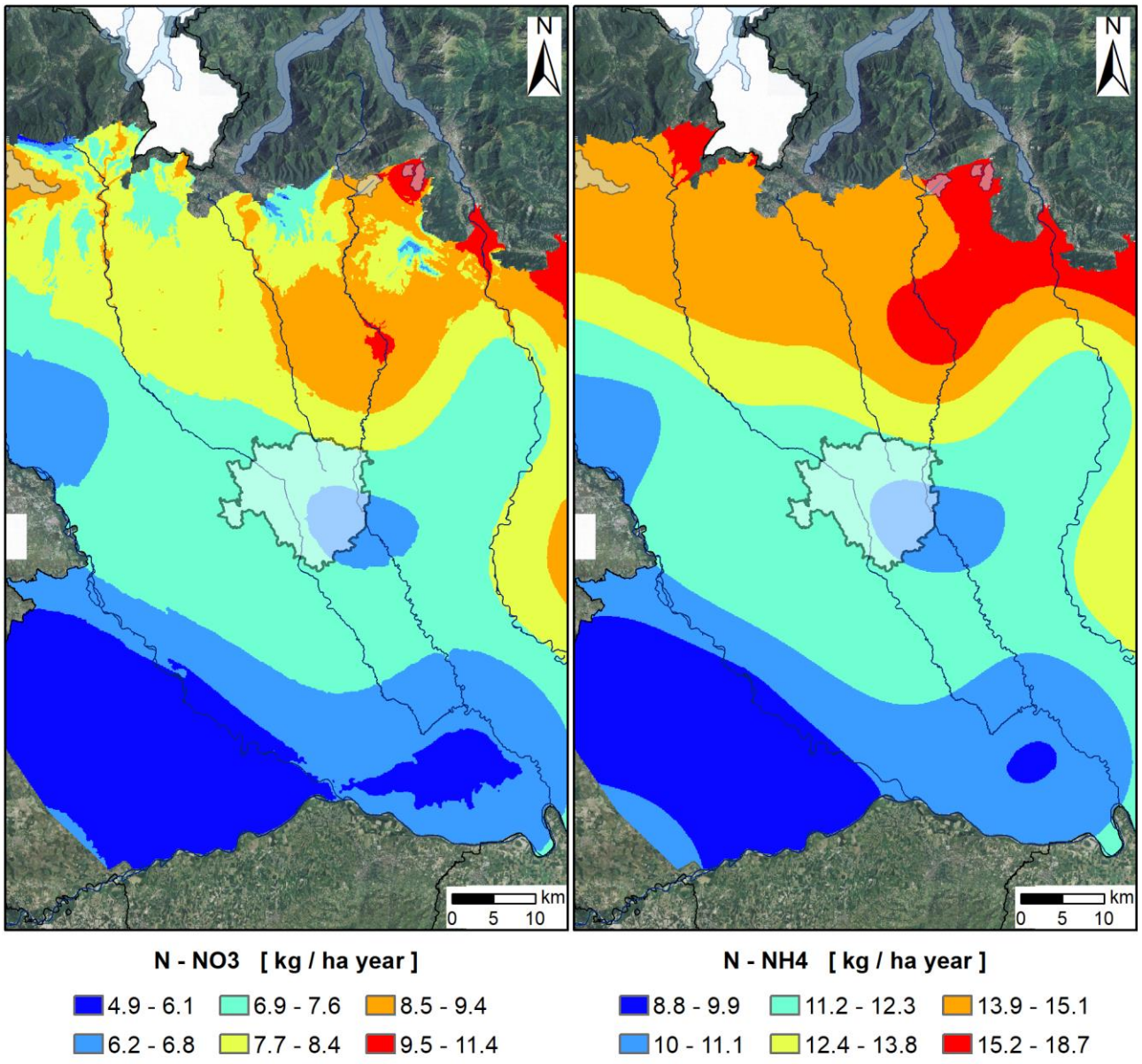

Figure 8 – Maps of N-NO_3^- depositions (left) and N-NH_4^+ depositions (right).

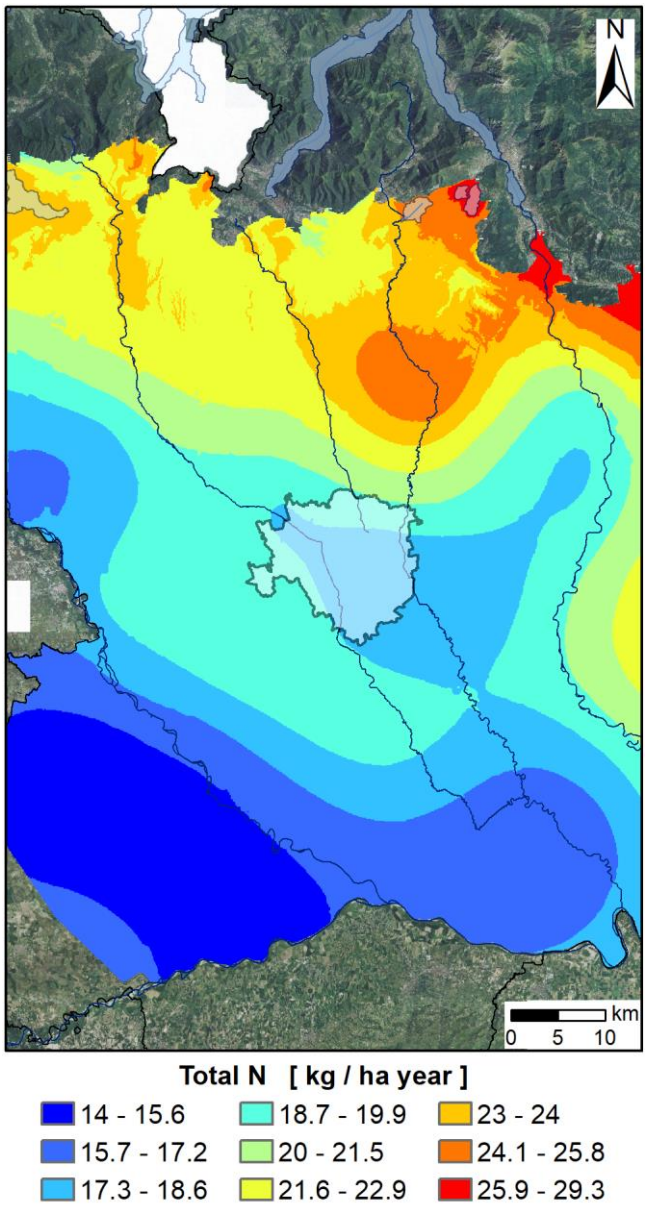

Figure 9 – Total N depositions obtained as a sum of N-NO_3^- and N-NH_4^+ depositions.

5 Discussion

Results showed by the map of total wet nitrogen deposition are extremely useful for the management of surface and subsurface ecosystems. Some sectors of the study area are used for agricultural activities: these sectors mainly cover the southern and the central western areas, even if some spots also occurs in the northern part. About the 33% of the total agricultural area is used for rice and 10% for alfalfa production, requiring 100-150 kg/ha/cycle and 25-30 kg/ha/cycle of nitrogen, respectively. This implies that the amount

of wet nitrogen deposition can locally reach a significant percentage of the total nitrogen required by the crop (15-25% for rice) or even almost totally cover this requirement (alfalfa). This result is relevant for those areas where farmers practice organic agriculture that is focused on precision farming. Consider that some farmers report that alfalfa is produced without the use of any fertilizers (e.g., Niccolò Reverdini - La Forestina, personal communication).

The study area hosts a variety of natural habitats including inland surface water, grasslands and forest. Some of them, such as the *Meso- and eutrophic Quercus woodland* and the *Broadleaved deciduous woodland* are diffuse in the southern sector, while others, such as the *Sub-atlantic semi-dry calcareous grassland,* the *Inland dune pioneer grasslands*, the *Inland dune siliceous grasslands* and the *Low and medium altitude hay meadows* occur in all the area. According to Bobbink and Hettelingh (2011) the critical loads for these habitats range from a minimum of 8-15 kg/ha/y for the *Inland dune pioneer grasslands* and the *Inland dune siliceous grasslands,* to a maximum of 20-30 kg/ha/y for the *Low and medium altitude hay meadows*. These values are generally lower or very close to wet nitrogen deposition values reported by this study, indicating that many natural habitats suffer from a N excess that may cause short to long term effects such as decline in diversity, nutrient imbalance and changes in soil processes (Bobbink and Hettelingh, 2011).

The study area is located within a Nitrate Vulnerable Zone by the European Union (Nitrate Directive, 91/676/EEC) and object of many specific studies (Sorichetta et al., 2013; Stevenazzi et al., 2017). A key issue for water and land use managers is the determination of the background value of nitrate in groundwater, which is difficult to define in areas with high anthropogenic impacts (e.g., Panno et al., 2006). Wet deposition maps can help in addressing this issue by identifying where the background values could be relatively higher and to what extent. Even if the latter could require intense numerical modelling activity of flow and nitrate transport in the vadose zone, the former can be efficiently addressed through a comparison with a nitrate groundwater vulnerability map (Stevenazzi et al., 2017). The overlay with the wet nitrogen deposition map highlights that significant changes in nitrate background values could be expected going from north to south. The northern area is the one where there is an overlap between most vulnerable areas and high wet nitrogen depositions while the opposite occurs in the southern sector (Figure 10). These distinctive combinations of

factors are strategically important in determining background values and support the scenario of adopting different background values according to the changes in natural and anthropogenic conditions across the area.

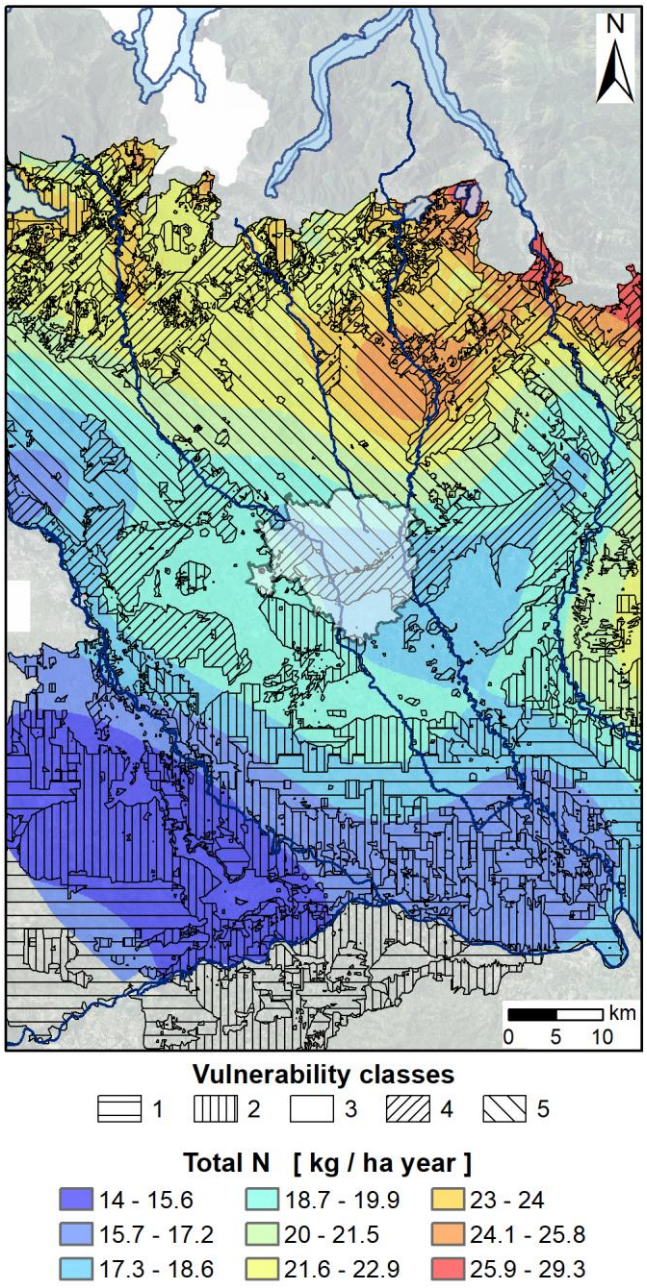

Figure 10 – Overlay between the total wet nitrogen deposition and groundwater vulnerability map to nitrate contamination in the study area from Stevenazzi et al., 2017. Vulnerability increases from class 1 to 5.

6 Conclusion

The study focused on rainfall chemistry characterization in a highly human impacted area with multiple land uses, to evaluate the implication of wet nitrogen deposition on surficial and subterranean ecosystems.

The results show that:

- although rainfall chemistry presents a clear spatial trend from north to south, nitrogen compounds (NO_3^-, NH_4^+) are always the most abundant components in rainwater samples;
- the presence of N compounds and their temporal variations in rainwater are consistent with pollution coming from local anthropogenic emission sources of NO_x and NH_3, mainly related to i) the use of the heating systems of residential and commercial buildings in the cold seasons, and ii) the spreading of fertilizers and manure on agricultural fields during the fertilization periods;
- a significant amount (from 14 to about 30 kg (N) ha^{-1} yr^{-1}) of wet nitrogen depositions over the entire area comes from rainfall and the contribution of ammonium is generally higher than the one of nitrate.

The main consequences are:

- many natural habitats characterizing the study area could have a short to long term negative evolution because they are suffering from an exceedance of nitrogen, as their critical load value is lower or very close to the calculated wet nitrogen deposition values;
- in some sectors, where many farmers share the practice of precision farming, the amount of wet nitrogen deposition can reach a significant percentage of the total nitrogen required by the crop;
- areas with significant nitrogen deposition values strongly coincide with high vulnerable areas to nitrate contamination in groundwater, thus determining a high probability of large background values of nitrate in groundwater.

These results are extremely helpful for supporting land use management and development to minimize the use of fertilizers in agriculture and the risk to deteriorate surficial ecosystems and groundwater.

7 Appendices

Appendix 1

Microwave plasma atomic emission spectroscopy (MP-AES) and ion chromatography (ICS) methods in measuring major cation concentrations have been compared applying the Bland-Altman graphical technique (Bland and Altman, 1999), which allows assessing the relative agreement between two laboratory analytical methods that measure the same chemical substance (Magari, 2002).

Figure S1a shows the measurements obtained by ICS plotted against those obtained through MP-AES, to assess visually how well the methods agree: data should lie along a straight line passing through the origin in a 45° angle (i.e., equality line). But, it seems that ICS results are slightly higher than MP-AES results. However, this plot can be misleading: the greater the range of measurements, the better the agreement will appear to be. Instead, measuring the differences between the two methods for each measurement plotted against their means and adding the limits of agreement (Figure A1b) is a better way of assessing the relationship, as it clearly shows the pattern of the individual differences. The mean difference is 0.07 mg/L and the standard deviation of the differences is 0.48 mg/L. Thus, the limits of agreement with a 95% confidence level are -0.86 mg/L and 1.01 mg/L (dashed lines in Figure A1b). Nonetheless, Figure S1b shows an increase in variability of the differences as the magnitude of the measurement increases. Thus, a logarithmic (i.e., natural logarithmic) transformation of both measurements has been applied.

Figure S2 shows the logarithmic transformed data and the difference versus mean plot with superimposed 95% limits of agreement. The range of values has been reduced and data lie along the “equality line” (Figure A2a). The mean difference (log ICS – log MP-AES) is 0.03 with 95% limits of agreement –0.071 and 0.076 (Figure A2b). Thus, it is possible to assure the agreement between ICS and MP-AES methods for measuring major cation concentration and that the two measurement methods can be used interchangeably.

It is important to note that instrumental errors are considered within the range of variability of differences between the two methods.

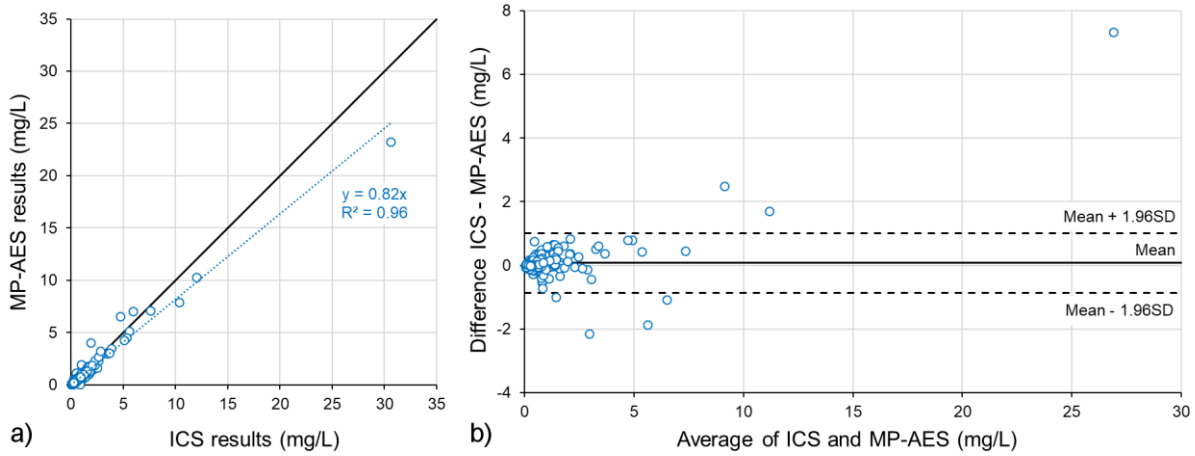

Figure A1 – a) Measurements of base cations concentrations; b) Plot of differences versus average with 95% limits of agreement (SD = standard deviation).

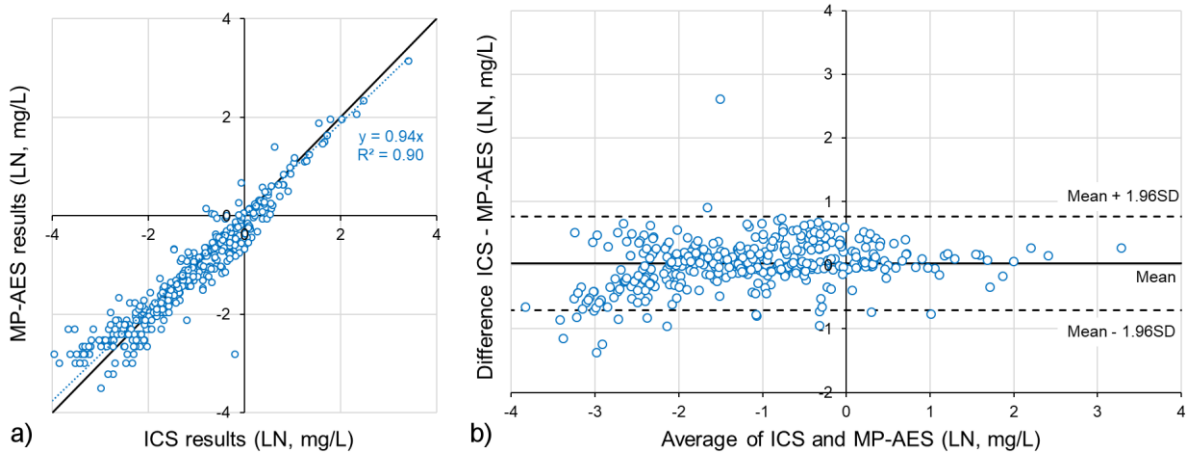

Figure A2 – a) Measurements of base cations concentrations after logarithmic transformation (LN = natural logarithm); b) Plot of differences versus average after logarithmic transformation with 95% limits of agreement (SD = standard deviation).

Appendix 2

a) Ionic balance. The completeness of measured parameters and the principle of electroneutrality in precipitation were checked through the ratio of total anions to that of cations. This ratio is expressed as (WMO/GAW, 2004; Equation A1):

$$\mathrm{BAL}(\%) = 100 \times \frac{\mathrm{CE} - \mathrm{AE}}{\mathrm{CE} + \mathrm{AE}} \quad \text{(Eq. A1)}$$

with CE and AE being the sum of cation and anions equivalents (meq/L), respectively, CE is the sum of Ca^{2+}, Na^{+}, Mg^{2+}, K^{+}, NH_4^{+} and H^{+}. AE is the sum of NO_3^{-}, NO_2^{-}, SO_4^{2-}, Cl^{-} and F^{-}. CE and AE are calculated as (WMO/GAW, 2004; Equation A2 and A3):

$$\mathrm{CE} = \left[\sum \frac{C_{Ci}}{(Eq.Wt.)_{Ci}}\right] + \frac{10^{(6-\mathrm{pH})}}{1000} \quad \text{(Eq. A2)}$$

$$\mathrm{AE} = \left[\sum \frac{C_{Ai}}{(Eq.Wt.)_{Ai}}\right] \quad \text{(Eq. A3)}$$

where C_{Ci} and C_{Ai} are the concentrations of the i^{th} cation (*C*) or anion (*A*) in mg/L, *Eq.Wt.* is the equivalent weight of the i^{th} cation (*C*) or anion (*A*), $10^{(6\text{-pH})}$ is the H^{+} concentration in meq/L.

The acceptability criterion was set as BAL ≤ ±20% to comply with the requirements of the Global Atmosphere Watch Program for precipitation chemistry (WMO/GAW, 2004) and according to previous works on precipitation quality (e.g., Balestrini et al., 2000; Yang et al., 2012).

b) Electric conductivity balance. Measured and calculated electric conductivities (EC) are compared according to Equation A4 (WMO/GAW, 2004).

$$\Delta\mathrm{EC}(\%) = 100 \cdot \frac{\mathrm{EC_c} - \mathrm{EC}}{\mathrm{EC}} \quad \text{(Eq. A4)}$$

where EC_C is the calculated electric conductivity and EC is the measured electric conductivity, both expressed as μS/cm. For dilute solutions, the total (calculated) conductivity can be calculated in μS/cm from the molar concentrations and molar ionic conductances of the individual ions, as follows (WMO/GAW, 2004; Equation A5):

$$\mathrm{EC_c} = \sum c_i \cdot \Lambda_i^{\circ} \quad \text{(Eq. A5)}$$

where EC_C is the calculated conductivity (μS/cm), c_i is the ionic concentration of the i^{th} ion (mmol/L) and Λ_i° the molaric ionic conductance of the i^{th} ion (Scm²/mol) at infinite solution and 25°C. Thus (Equation A6):

$$\mathrm{EC_C} = 10^{(3-\mathrm{pH})} \cdot 349.7 + \mathrm{c}[\mathrm{F^-}] \cdot + \mathrm{c}[\mathrm{Cl^-}] \cdot 76.3 + \mathrm{c}[\mathrm{NO_2^-}] \cdot 71.8 + \mathrm{c}[\mathrm{NO_3^-}] \cdot 71.4 + \mathrm{c}[\mathrm{SO_4^{2-}}] \cdot 160 + \mathrm{c}[\mathrm{Ca^{2+}}] \cdot 119 + \mathrm{c}[\mathrm{Mg^{2+}}] \cdot 106 + \mathrm{c}[\mathrm{Na^+}] \cdot 50.1 + \mathrm{c}[\mathrm{K^+}] \cdot 73.5 + \mathrm{c}[\mathrm{NH_4^+}] \cdot 73.5 \quad \text{(Eq. A6)}$$

where $10^{(3\text{-pH})}$ expresses the concentration of H^+.

The acceptability criterion was set as $\Delta EC \leq \pm 30\%$ to comply with the requirements of the Global Atmosphere Watch Program for precipitation chemistry (WMO/GAW, 2004) and according to previous works on precipitation quality (e.g., Balestrini et al., 2000; Yang et al., 2012).

c) Marine inputs. The sea salt fraction (SSF) and the non-sea salt fraction (NSSF) are calculated according to Keene et al. (1986; WMO/GAW, 2004) by comparing ionic ratios in rainwater and seawater using sodium as the reference species (e.g., Moreda-Piñeiro et al., 2014; Deusdará et al., 2017), following Equation A7 and A8.

$$\%(\mathrm{SSF})_X = \frac{100 \cdot (Na)\left(\frac{X_{sea}}{Na_{sea}}\right)}{X} \quad \text{(Eq. A7)}$$

$$\%(\mathrm{NSSF})_X = 100 - \%(\mathrm{SSF})_X \quad \text{(Eq. A8)}$$

where *X* is the concentration of ions as measured in rainwater, X_{sea} is the concentration of the sea water ions and Na_{sea} is the concentration of Na^+ taken as a reference in sea water. All concentrations are expressed in meq/L.

d) Neutralization factors. The acidity of rainwater potentially originates from the dissociation of nitric and sulphuric acids anions (NO_3^- and SO_4^{2-}) that are neutralized by alkaline species, such as Ca^{2+}, Mg^{2+}, K^+ and NH_4^+as well as on the neutralization reactions among them (e.g., Moreda-Piñeiro et al., 2014; Deusdará et al., 2017). The neutralization factor (NF) is expressed as shown in Equation A9.

$$\mathrm{NF}_x = \frac{[X]}{[\mathrm{NO_3^-} + \mathrm{SO_4^{2-}}]} \quad \text{(Eq. A9)}$$

where [*X*] is the concentration of the species responsible for neutralization (Ca^{2+}, Mg^{2+}, K^+, NH_4^+). The volume weighted mean for each species, expressed as meq/L, is used for the calculation of the neutralization factors.

e) Descriptive statistics are calculated for ionic concentrations, EC and pH values: arithmetic mean, volume weighted mean, median, minimum and maximum values and standard deviation. Volume weighted mean (VWM) was calculated by using Equation A10. It allows taking into account the effect of dilution by the rain amount and is useful in comparative studies.

$$\mathrm{VWM} = \frac{\sum_{i=1}^{N} v_i [X_i]}{\sum_{i=1}^{N} v_i} \qquad \text{(Eq. A10)}$$

where $[X_i]$ is the concentration of ion *X* or the value of parameter *X* (i.e., pH and EC), v_i is the water sample volume and *N* is the number of samples. Concentration can be expressed as mg/L, meq/L or μeq/L. pH has no unit of measure. EC is expressed as μS/cm.

8 References

1. Amato F., Alastuey A., Karanasiou A., Lucarelli F., Nava S., Calzolai G., et al., 2016. AIRUSE-LIFE+: a harmonized PM speciation and source apportionment in five southern European cities. Atmospheric Chemistry and Physics, vol. 16(5), pp. 3289–3309, doi: 10.5194/acp-16-3289-2016
2. Balestrini R., Galli L., Tartari G., 2000. Wet and dry atmospheric deposition at prealpine and alpine sites in northern Italy. Atmospheric Environment, vol. 34(9), pp. 1455-1470, doi: 10.1016/S1352-2310(99)00404-5
3. Bland J.M., Altman D.G., 1999. Measuring agreement in method comparison studies. Statistical Methods in Medical Research, 8:135-160
4. Berkowicz R., Palmgren F., Hertel O., Vignati E., 1996. Using measurements of air pollution in streets for evaluation of urban air quality - Meterological analysis and model calculations. Science of the Total Environment, vol. 189-190, pp. 259-265, doi: 10.1016/0048-9697(96)05217-5
5. Bland J.M., Altman D.G., 1999. Measuring agreement in method comparison studies. Statistical Methods in Medical Research, vol. 8, pp. 135-160
6. Bobbink R., Hettelingh J.P., 2011. Review and revisions of empirical critical loads and dose–response relationships. Proceedings of an expert workshop, Noordwijkerhout 23–24 June 2010, Bilthoven, the Netherlands, RIVM
7. Brimblecombe, P. (2003). 8.14 - The Global Sulfur Cycle. In H. D. Holland & K. K. Turekian (Eds.), Treatise on Geochemistry (pp. 645–682). Oxford: Pergamon. doi: 10.1016/B0-08-043751-6/08134-2
8. Brunetti M., Buffoni L., Maugeri M., Nanni T., 2000. Precipitation intensity trends in northern Italy. International Journal of Climatology: A Journal of the Royal Meteorological Society, vol. 20(9), pp. 1017-1031
9. Buoli M., Grassi S., Caldiroli A., Carnevali G.S., Mucci F., Iodice S., Cantone L., Pergoli L., Bollati V., 2018. Is there a link between air pollution and mental disorders? Environment International, vol. 118, pp. 154-168, doi: 10.1016/j.envint.2018.05.044
10. Carnevale C., Decanini E., Volta M., 2008. Design and validation of a multiphase 3-D model to simulate tropospheric pollution, Sci. Total Environ., vol. 390, pp. 166-176, doi: 10.1016/j.scitotenv.2007.09.017
11. Celle-Jeanton H., Travi Y., Loÿe-Pilot M.-D., Huneau F., Bertrand G., 2009. Rainwater chemistry at a Mediterranean inland station (Avignon, France): Local contribution versus long-range supply. Atmospheric Research, vol. 91, pp.118-126, doi: 10.1016/j.atmosres.2008.06.003
12. Ceriani M., Carelli M., 2003. Carta delle precipitazioni medie, massime e minime annue del territorio alpino della Regione Lombardia (registrate nel periodo 1891-1990). Pubblicazione Regione Lombardia

13. Charlson R.J., Rhode J., 1982. Factors controlling the acidity of natural rainwater. Nature vol. 295, pp. 683-685
14. Deusdará K.R.L., Forti M.C., Borma L.S., Menezes R.S.C., Lima J.R.S., Ometto J.P.H.B., 2017. Rainwater chemistry and bulk atmospheric deposition in a tropical semiarid ecosystem: the Brazilian Caatinga. J. Atmos. Chem., vol. 74(1), pp. 71-85, doi: 10.1007/s10874-016-9341-9
15. Dosio A., Galmarini S., Graziani G., 2002. Simulation of the circulation and related photochemical ozone dispersion in the Po plains (northern Italy): Comparison with the observations of a measuring campaign. J. Geophys. Res., vol. 107(D18), 8189, doi: 10.1029/2000JD000046
16. European Community, 1991. Council Directive 91/676/EEC concerning the protection of waters against pollution caused by nitrates from agricultural sources, (Nitrate Directive). OJ L 375, 31 December 1991, pp. 1-8
17. European Community, 2008. Directive 2008/50/EC of the European Parliament and of the Council of 21 May 2008 on ambient air quality and cleaner air for Europe. OJ L 152, 11 June 2008, pp. 1-44
18. EEA – European Environment Agency, 2018. European Union emission inventory report 1990-2016 under the UNECE Convention on Long-range Transboundary Air Pollution (LRTAP). EEA Report No 6/2018, pp. 150, doi: 10.2800/571876
19. EMEP/CEIP, 2018. EMEP Emissions Data. European Monitoring and Evaluation Programme/Centre on Emission Inventories and Projections. Available at: http://www.ceip.at/
20. ESA, 2019a. Nitrogen dioxide pollution mapped. European Space Agency, news released on 12 March 2019. Available at: http://www.esa.int/Our_Activities/Observing_the_Earth/Copernicus/Sentinel-5P/Nitrogen_dioxide_pollution_mapped
21. ESA, 2019b. The air we breathe. European Space Agency, news released on 16 May 2019. Available at: http://www.esa.int/Our_Activities/Observing_the_Earth/Copernicus/Sentinel-5P/The_air_we_breathe2
22. Galloway J.N., Lickens G.E., Keene W.C., Miller J.M., 1982. The composition of precipitation in remote areas of the world. Journal of Geophysical Research, vol. 87, pp. 8771-8786
23. Galloway J.N., Townsend A.R., Erisman J.W., Bekunda M., Cai Z., Freney J.R., Martinelli L.A., Seitzinger S.P., Sutton M.A., 2008. Transformation of the Nitrogen Cycle: Recent Trends, Questions, and Potential Solutions. Science, vol. 320(5878), pp. 889-892, doi: 10.1126/science.1136674
24. Gómez-Carracedo M.P., Andrade J.M., Ballabio D., Prada-Rodríguez D., Muniategui-Lorenzo S., Consonni V., Piñeiro-Iglesias M., López-Mahía P., 2015. Impact of medium-distance pollution sources in a Galician suburban site (NW

Iberian peninsula). Science of the Total Environment, vol. 512-513, pp. 114-124, doi: 10.1016/j.scitotenv.2015.01.029

25. Grimshaw H.J., Dolske D.A., 2002. Rainfall concentrations and wet atmospheric deposition of phosphorus and other constituents in Florida, U.S.A. Water, Air, and Soil Pollution, vol. 137(1–4), pp. 117-140, doi: 10.1023/A:1015505624739
26. Ham Y.S., Tamiya S., 2006. Contribution of dissolved organic nitrogen deposition to total dissolved nitrogen deposition under intensive agricultural activities. Water Air Soil Pollution, vol. 178(1-4), pp. 5-13, doi: 10.1007/s11270-006-9109-y
27. ISPRA - Istituto Superiore per la Protezione e la Ricerca Ambientale, 2016. Focus su inquinamento atmosferico nelle aree urbane ed effetti sulla salute, Stato dell'ambiente 68/2016
28. Keene W.C., Pszenny A.P., Galloway J.N., Hawley M.E., 1986. Sea salt corrections and interpretations of constituent ratios in marine precipitation. J. Geophys. Res. vol. 91, pp. 6647-6658
29. Kennedy F., 2001. How extensive are the impacts of nitrogen pollution in Great Britain's forests? Forest Research Annual Report 2001/2, pp. 66-75
30. Kim K.H., Yun S.T., Kim H., Kim J., 2015. Determination of natural backgrounds and thresholds of nitrate in South Korean groundwater using model-based statistical approaches. J. Geochem. Explor., vol. 148, pp. 196-205, doi: 10.1016/j.gexplo.2014.10.001
31. Lee D.S., Kingdon R.D., Pacyna J.M., Bouwman A.F., Tegen I., 1999. Modelling base cations in Europe—sources, transport and deposition of calcium. Atmospheric Environment, vol. 33(14), pp. 2241-2256, doi: 10.1016/S1352-2310(98)00169-1
32. Magari M.T., 2002. Statistics for Laboratory Method Comparison Studies. Bio Pharm, 15(1):28-32
33. Meyer S.T., Koch C., Weisseret W.W., 2015. Towards a standardized Rapid Ecosystem Function Assessment (REFA). Trends in Ecology & Evolution, vol. 30, pp. 390-397, doi: 10.1016/j.tree.2015.04.006
34. Moreda-Piñeiro J., Alonso-Rodríguez E., Moscoso-Pérez C., Blanco-Heras G., Turnes-Carou I., López-Mahía P., Muniategui-Lorenzo S., Prada-Rodríguez D., 2014. Influence of marine, terrestrial and anthropogenic sources on ionic and metallic composition of rainwater at a suburban site (northwest coast of Spain). Atmos. Environ., vol. 88, pp. 30-38, doi: 10.1016/j.atmosenv.2014.01.067
35. Mosello R., Tartari G.A., 1992. Formiate and acetate in wet deposition at Pallanza (NW Italy) in relation to major ion concentrations. Water, Air and Soil Pollution 63, pp. 397-409

36. NASA Hyperwall, 2018. Nitrogen Dioxide from Aura/OMI, 2017-2018. Available at: https://svs.gsfc.nasa.gov/30986
37. Naselli-Flores L., 2010. Mediterranean Climate and Eutrophication of Reservoirs: Limnological Skills to Improve Management. In: Ansari A., Singh Gill S., Lanza G., Rast W. (eds) Eutrophication: causes, consequences and control. Springer, Dordrecht, pp. 131-142
38. Ochoa-Hueso R., Allen E.B., Branquinho C., Cruz C., Dias T., Fenn M.E., et al., 2011. Nitrogen deposition effects on Mediterranean-type ecosystems: An ecological assessment. Environmental Pollution, vol. 159(10), pp. 2265-2279, doi: 10.1016/j.envpol.2010.12.019
39. Ordóñez C., Richter A., Steinbacher M., Zellweger C., Nüß H., Burrows J.P., Prévôt A.S.H., 2006. Comparison of 7 years of satellite-borne and ground-based tropospheric NO_2 measurements around Milan, Italy. J. Geophys. Res., vol. 111, D05310, doi: 10.1029/2005JD006305
40. Panettiere P., Cortecci G., Dinelli E., Bencini A., Guidi M. 2000. Chemistry and sulfur isotopic composition of precipitation at Bologna, Italy. Applied Geochemistry, vol. 15 (10), pp. 1455-1467, doi: 10.1016/S0883-2927(00)00012-3
41. Panno S.V., Kelly W.R., Martinsek A.T., Hackley K.C., 2006. Estimating background and threshold nitrate concentrations using probability graphs. Ground Water, vol. 44(5), pp. 697-709, doi: 10.1111/j.1745-6584.2006.00240.x
42. Payne R.J., Dise N.B., Stevens C.J., Gowing D.J., and BEGIN Partners, 2013. Impact of nitrogen deposition at the species level. PNAS, vol. 110(3), pp. 984-987, doi: 10.1073/pnas.1214299109
43. Peel M.C., Finlayson B.L., McMahon T.A., 2007. Updated world map of the Köppen-Geiger climate classification. Hydrology and Earth System Sciences, vol. 11, pp. 1633–1644
44. Rattigan O.V., Civerolo K. L., Felton H.D., 2017. Trends in wet precipitation, particulate, and gas-phase species in New York State. Atmospheric Pollution Research, vol. 8(6), pp. 1090–1102, doi: 10.1016/j.apr.2017.04.007
45. Rogora M., Arisci S., Marchetto A., 2012. The role of nitrogen deposition in the recent nitrate decline in lakes and rivers in Northern Italy. Science of the Total Environment, vol. 417–418, pp. 214-223, doi: 10.1016/j.scitotenv.2011.12.067
46. Rogora M., Colombo L., Marchetto A., Mosello R., Steingruber S., 2016. Temporal and spatial patterns in the chemistry of wet deposition in Southern Alps. Atmospheric Environment, vol. 146, pp. 44-54, doi: 10.1016/j.atmosenv.2016.06.025

47. Schindler D.W., 2006. Recent advances in the understanding and management of eutrophication. Limnol. Oceanogr., vol. 51(1), pp. 356-363, doi: 10.4319/lo.2006.51.1_part_2.0356
48. Sorichetta A., Ballabio C., Masetti M., Robinson G.R. Jr., Sterlacchini S., 2013. A comparison of data-driven groundwater vulnerability assessment methods. Ground Water, vol. 51(6), pp. 866-879, doi: 10.1111/gwat.12012
49. Steingruber S., 2015. Acidifying Deposition in Southern Switzerland. Monitoring, Maps and Trends 1988-2013. Ufficio dell'aria, del clima e delle energie rinnovabili, Dipartimento del territorio del Canton Ticino, Bellinzona, pp. 60
50. Stevenazzi S., Nghiem S.V., Masetti M., 2015. Urban impacts on air quality observed with remote sensing and ground station data from the Po Plain Field Campaign. In: IEEE Geoscience and Remote Sensing Symposium, Milan (Italy), pp. 73-75, ISBN: 978-1-4799-7928-8
51. Stevenazzi S., Masetti M., Beretta G.P., 2017. Groundwater vulnerability assessment: from overlay methods to statistical methods in the Lombardy Plain area. Acque Sotterranee - Italian Journal of Groundwater, vol. 6, pp. 17-27, doi: 10.7343/as-2017-276
52. Sutton M.A., Howard C.M., Erisman J.W., Billen G., Bleeker A., Grennfelt P., van Grinsven H., Grizzeti B., 2011. The European Nitrogen Assessment: sources, effects and policy perspectives. Cambridge University Press, pp. 612
53. Van Damme M., Clarisse L., Whitburn S., Hadji-Lazaro J., Hurtmans D., Clerbaux C., Coheur P.-F., 2018. Industrial and agricultural ammonia point sources exposed. Nature, vol. 564(7734), pp. 99, doi: 10.1038/s41586-018-0747-1
54. Vet R., Artz R.S., Carou S., Shaw M., Ro C.-U., Aas W., Baker A., Bowersox Van C., Dentener F., Galy-Lacaux C., Hou A., Pienaar J.J., Gillett R., Forti M.C., Gromov S., Hara H., Khodzher T., Mahowald N.M., Nickovic S., Rao P.S.P., Reid N.W., 2014. A global assessment of precipitation chemistry and deposition of sulfur, nitrogen, sea salt, base cations, organic acids, acidity and pH, and phosphorus. Atmospheric Environment, vol. 93, pp. 3-100, doi: 10.1016/j.atmosenv.2013.10.060
55. Williams J.J., Lynch J.A., Saros J.E., Labou S.G., 2017. Critical loads of atmospheric N deposition for phytoplankton nutrient limitation shifts in western US mountain lakes. Ecosphere, vol. 8(10), e01955, doi: 10.1002/ecs2.1955
56. WMO/GAW, 2004. Manual for the GAW Precipitation Chemistry Programme: Guidelines, Data Quality Objectives and Standard Operating Procedures. No. 160. World Meteorological Organization/Global Atmosphere Watch, Geneva, Switzerland
57. Xiao H.-W., Xiao H.-Y., Long A.-M., Wang Y.-L., Liu C.-Q., 2013. Chemical composition and source apportionment of rainwater at Guiyang, SW China. J. Atmos. Chem., vol. 70, pp. 269-281, doi: 10.1007/s10874-013-9268-3

58. Yang F., Tan J., Shi Z.B., Cai Y., He K., Ma Y., Duan F., Okuda T., Tanaka S., Chen G., 2012. Five-year record of atmospheric precipitation chemistry in urban Beijing, China. Atmos. Chem. Phys., vol. 12, pp. 2025-2035, doi: 10.5194/acp-12-2025-2012